2021 43rd Annual International Conference of the
IEEE Engineering in Medicine & Biology Society (EMBC)
Oct 31 - Nov 4, 2021. Virtual Conference

Ultrasound Echogenicity-based Assessment of Muscle Fatigue During Functional Electrical Stimulation

Qiang Zhang, Ashwin Iyer, Krysten Lambeth, Kang Kim, and Nitin Sharma*

***Abstract*—The rapid onset of muscle fatigue during functional electrical stimulation (FES) is a major challenge when attempting to perform long-term periodic tasks such as walking. Surface electromyography (sEMG) is frequently used to detect muscle fatigue for both volitional and FES-evoked muscle contraction. However, sEMG contamination from both FES stimulation artifacts and residual M-wave signals requires sophisticated processing to get clean signals and evaluate the muscle fatigue level. The objective of this paper is to investigate the feasibility of computationally efficient ultrasound (US) echogenicity as a candidate indicator of FES-induced muscle fatigue. We conducted isometric and dynamic ankle dorsiflexion experiments with electrically stimulated tibialis anterior (TA) muscle on three human participants. During a fatigue protocol, we synchronously recorded isometric dorsiflexion force, dynamic dorsiflexion angle, US images, and stimulation intensity. The temporal US echogenicity from US images was calculated based on a gray-scaled analysis to assess the decrease in dorsiflexion force or motion range due to FES-induced TA muscle fatigue. The results showed a monotonic reduction in US echogenicity change along with the fatigue progression for both isometric ($R^2 = 0.870 \pm 0.026$) and dynamic ($R^2 = 0.803 \pm 0.048$) ankle dorsiflexion. These results implied a strong linear relationship between US echogenicity and TA muscle fatigue level. The findings indicate that US echogenicity may be a promising computationally efficient indicator for assessing FES-induced muscle fatigue and may aid in the design of muscle-in-the-loop FES controllers that consider the onset of muscle fatigue.**

I. Introduction

Human ankle dorsiflexion plays an essential role during lower limb functionalities, especially for ground clearance during the walking swing phase [1]. Neurological disorders, like stroke and multiple sclerosis, are very likely to impede ankle dorsiflexion movement, known as drop foot. Patients with drop foot lack normal foot ground clearance, which results in unnatural steppage gait to avoid tripping/falling [2]. Functional electrical stimulation (FES) has been widely used in recent decades to address drop foot [3]–[5]. However, due to the non-selective stimulation nature of FES, peripheral motor units are synchronously activated and discharged, resulting in a rapid onset of muscle fatigue that decreases the force generated from the muscle contraction, which usually causes the loss of FES control effectiveness [6].

The deficiency of direct measurement of muscle fatigue limits the quantitative assessment of the fatigue influence on the FES-elicited neuromusculoskeletal dynamic system and impedes the adaptive FES controller design. Efforts in indirectly measuring fatigue include but are not limited to tetanic contraction force measurement [7], electromyography (EMG) / surface electromyography (sEMG) [8]–[10], mechanomyography [11], near-infrared spectroscopy [12], [13], and phosphorus nuclear magnetic resonance [14]. Among these technologies, sEMG is the most well-developed and convenient non-invasive methodology to assess peripheral muscle fatigue. Although significant contributions in volitional sEMG extraction during FES have been reported in [15], [16], the analysis and evaluation of FES-elicited muscle fatigue based on the extracted volitional sEMG signals are still challenging, mainly due to 1) FES-induced contractions cluttering and masking the pure sEMG signals [17], [18], 2) interference and cross talk from adjacent muscles [9], and 3) the inability to measure deeply located muscles [19]. Recently, ultrasound (US) imaging has been investigated to assess muscle fatigue for volitional and FES-induced muscle contraction as an alternative to EMG. Due to the relatively high spatial and temporal resolution, the US images can provide a direct visualization of muscle contraction deformation during fatigue and a comprehensive measure to reflect the fatigue effect. Shi et al. [20] used muscle thickness extracted from cross-sectional US images to characterize the biceps brachii muscles' behaviors during fatigue caused by volitional isometric contraction for a long duration. Witte et al. [21] applied US strain imaging to capture the elastic and viscoelastic-like modifications in the 3^{rd} flexor digitorum superficialis muscle after a fatiguing exercise. Sheng et al. [22] investigated an adaptive speckle tracking algorithm to assess the quadriceps contraction strain change to evaluate muscle fatigue induced by FES under isometric knee extension.

The aforementioned US imaging-related studies for as-

Q. Zhang, A. Iyer, K. Lambeth, and N. Sharma are with the UNC/NC State Joint Department of Biomedical Engineering, NC State University, Raleigh, NC 27695 USA (e-mail: qzhang25@ncsu.edu; aiyer3@ncsu.edu; kflambet@ncsu.edu; kangkim@upmc.edu; nsharm23@ncsu.edu).

K. Kim is with the Department of Bioengineering, School of Engineering, University of Pittsburgh, Pittsburgh, PA 15260 USA, with the Center for Ultrasound Molecular Imaging and Therapeutics, Department of Medicine and Heart and Vascular Institute, University of Pittsburgh School of Medicine and University of Pittsburgh Medical Center, Pittsburgh, PA 15213 USA, with the Department of Mechanical Engineering and Materials Science, School of Engineering, University of Pittsburgh, Pittsburgh, PA 15260 USA, and also with the McGowan Institute for Regenerative Medicine, University of Pittsburgh and University of Pittsburgh Medical Center, Pittsburgh, PA 15219 USA (e-mail: kangkim@upmc.edu). (*Corresponding author: Nitin Sharma). This work was funded by NSF CAREER Award # 1750748.

sessing muscle fatigue were all based on isometric muscle contractions, and few studies have considered dynamic motion. Additionally, the US imaging characteristics extraction methods in these studies were computationally intensive, which impedes the real-time implementation. Inspired by recent work in US imaging to detect changes in muscle contractility [23], [24], we investigated the feasibility of using the computationally efficient US echogenicity to quantitatively assess FES-induced tibialis anterior (TA) muscle fatigue during both isometric and dynamic ankle dorsiflexion movements. We synchronously collected dorsiflexion force, dorsiflexion angle, TA muscle US images, and FES intensity during the muscle fatigue progression for both isometric and dynamic cases from three human participants without neurological disorders. The temporal US echogenicity feature within the image region of interest (ROI) was calculated based on a gray-scaled analysis as mentioned in [23]. A comprehensive correlation analysis between the temporal US echogenicity relative change (ERC) and TA muscle fatigue progression (decay of dorsiflexion force or angle during isometric or dynamic scenarios) was performed to assess the muscle contractility during fatigue progression. It is hypothesized that there exists a nonlinear relationship (exponential function) between the US ERC and the duration of applied FES, as well as a linear relationship between the US ERC and the decay of dorsiflexion force or angle. Furthermore, the performance of US ERC as a surrogate metric of muscle fatigue was compared to US tissue strain that was derived by a speckle tracking algorithm [22].

II. Methods and Apparatus

A. Experimental protocol and data collection

The study was approved by the Institutional Review Board (IRB) at North Carolina State University (IRB approval number: 20602). Three able-bodied participants without any neuromuscular disorders were recruited to complete FES-elicited ankle dorsiflexion experiments. Every participant signed an informed consent form before participating in the experiments. The isometric and dynamic experimental setup is illustrated in Fig. 1. Detailed descriptions of the isometric setup, including the load cell platform and US imaging machine, can be found in [24], [25]. In the dynamic experimental setup, the participant's foot was released from the load cell platform, and a wearable ankle brace connected with an incremental encoder was inserted into the participant's shoe. This seated posture was maintained throughout the entire experimental procedure. Two electrodes (size: 2"×2") were placed on the fibular head and the distal belly of the TA muscle, respectively, and used to pass the bi-phase stimulation pulse trains from a stimulator (Rehastim 2, HASOMED GmbH, Germany). A targeted region approximately 30% to 50% of individual shank length distal from the knee joint was chosen as the location for the US transducer placement, and depth of US imaging was set as 40 mm to include the entire TA muscle area.

There were three separate experimental sets on three different days, during which participants were instructed to

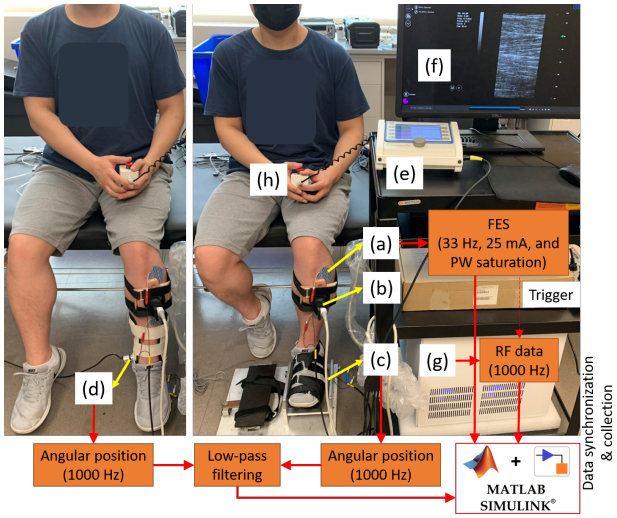

Figure 1: Illustration of isometric (right) and dynamic (left) experimental setup. a-FES electrode pads. b-Prodigy US transducer. c-Load cell platform. d-Incremental encoder. e-FES stimulator. f-B-mode US imaging screen. g-Prodigy US machine. h-Safety stop button.

avoid any volitional TA muscle contraction. The first set on the first day was performed to determine subject-specific system identification parameters, while the second and third sets were performed randomly on two days to analyze muscle fatigue in both isometric and dynamic scenarios. At least 72 hours were given between sets for each participant to have a full recovery and to mitigate muscle fatigue effects from the previous set. For both isometric and dynamic ankle dorsiflexion experiments, stimulation pulse trains with 25 mA current amplitude and 33 Hz stimulation frequency were commonly applied for all participants while stimulation pulse width was selected individually (400 μs, 500 μs, and 450 μs for three participants). In the first set, following the procedures described in [26], the threshold and saturation pulse widths for each participant were determined under the isometric case, and 80% of an individual's saturation pulse width was applied throughout the second and third sets. Two fatigue progression periods of 120 seconds and 240 seconds (FES was activated every 2 seconds with a duty cycle of 65%) were applied for the isometric case and dynamic case, respectively. Under the isometric and dynamic fatigue progressions, the dorsiflexion force signal and dorsiflexion angle signal were collected at 1000 Hz throughout the entire period, respectively. During the stimulation of both fatigue progressions, plane-wave US images were collected at 1000 frames per second to image 1 complete muscle contraction for every 4 FES stimulation cycles. The aforementioned experimental and data collection procedures were applied on both ankle joints of each participant.

B. Data processing and analysis

The ankle dorsiflexion force and angle measurements were low-pass filtered by a 4^{th}-order Butterworth filter with a cut-

off frequency of 5 Hz. After the US imaging radio frequency (RF) data was beamformed to get B-mode image sequences using MATLAB (R2018b, Mathworks, MA, USA), the first frame in every imaged contraction was subtracted from all of the subsequent images, and the resultant difference image was spatially filtered by a median filter and non-local means denoising [27]. The brightness of each difference image represents the normalized gray-scaled value (between 0 and 255) of each pixel. The ROI was selected with a depth from 5 mm to 35 mm to include most of the section of the bipennate TA muscle. The temporal US ERC in the same contraction was calculated as the mean gray-scaled value from the difference image time sequence. Given the FES-induced fatigue progression protocol, the time period during which US images were captured could guarantee the submaximal dorsiflexion force or motion to be reached after a transient muscle activation period; therefore, the final measure from dorsiflexion force or angle during each FES-elicited muscle contraction, along with the final measure from ERC during each US imaging-recorded muscle contraction, were selected to characterize the muscle contractility during fatigue progression. Therefore, during the isometric fatigue progression, 60 samples from dorsiflexion forces and 15 samples from ERC were obtained, while during the dynamic fatigue progression, 120 samples from the dorsiflexion angles and 30 samples from ERC were obtained. Then, the samples of each signal were normalized to the corresponding first sample, and all resultant values were between 0 and 1.

According to the muscle fatigue dynamics and its solution mentioned in [6], an exponential regression model was used to fit the curve between the normalized submaximal dorsiflexion force or motion and the index number of contractions ($i = 1, 2, ..., 60$/$i = 1, 2, ..., 120$), as well as the curve between the normalized submaximal ERC and the index number of contractions ($i = 4, 8, ..., 60$/$i = 4, 8, ..., 120$). The coefficients of the exponential regression models were determined by using the Levenberg-Marquardt nonlinear least squares algorithm. A linear regression model was used to fit the line between the normalized down-sampled submaximal dorsiflexion force or motion and the normalized submaximal ERC. The coefficient of determination (R^2) of each regression model was also calculated to evaluate the goodness of fitting. A paired t-test was performed on each of the linear and nonlinear model coefficients, where the optimal coefficient value was compared to zero with a p-value selected as 0.05. Similarly, a paired t-test was used to determine if there was a significant difference between R^2 values under isometric and dynamic cases. The significant difference level was chosen as $p < 0.05$.

III. Results and Discussion

A. Effects of fatigue on isometric and dynamic dorsiflexion

Figure 2 shows the representative FES-induced TA muscle fatigue's effects on the isometric dorsiflexion force normalization, dynamic dorsiflexion motion normalization, and TA muscle US ERC normalization, where the data are from the right ankle joint of participant A1. Remarkably, all signals show a monotonic decay trend with the muscle fatigue progression. The exponential regression model's equations and R^2 values are labeled in each subplot. In Fig. 2a, the submaximal dorsiflexion force reduces to 50% of the pre-fatigue value after about 35 contraction cycles, while the submaximal dorsiflexion angle reduces to 65% of the pre-fatigue value after about 65 contraction cycles. The results indicate that dynamic ankle dorsiflexion requires more FES repetitions than the isometric case to reach the same TA muscle fatigue level. In Fig. 2b, the decay of US ERC under isometric dorsiflexion is smoother than that under the dynamic case. Across the three participants, the exponential regression models present R^2 values of 0.917 ± 0.032 (mean$\pm$standard deviation) and 0.904 ± 0.047 between the normalized dorsiflexion force/normalized US ERC and contraction cycles under the isometric case, respectively, as well as R^2 values of 0.851 ± 0.039 and 0.753 ± 0.059 between normalized dorsiflexion angle/normalized US ERC and contraction cycles under the dynamic case, respectively. It is clear that the isometric fatigue progression causes a significantly stronger exponential relationship between the normalized dorsiflexion force ($p < 0.001$)/normalized US ERC ($p < 0.001$) and contraction cycles than the dynamic fatigue progression. By taking the dorsiflexion force and angle reduction as the muscle fatigue benchmark for the isometric and dynamic scenarios, the results from Fig. 2 present the potentials of the normalized US ERC as an alternatively and commonly effective muscle fatigue indicator.

B. Implication of US echogenicity as a fatigue indicator

Figure 3 presents the representative scatter plots between the TA muscle's US ERC normalization vs. dorsiflexion force normalization/angle normalization under isometric/dynamic fatigue progressions, where the data were collected from the left ankle joint of participant A2. The direction of decreasing force or angle corresponds to the fatigue progression direction, as labeled in Fig. 3. Through a linear regression model (the equations and R^2 values as shown in Fig. 3), strong linear relationships between the US ERC and dorsiflexion force/angle were observed with the p-value of each slope from the F-statistic less than 10^{-6}, which indicates US ERC is a reliable alternative fatigue indicator. To generalize the observed results in this trial, a summary of R^2, slope with p-value, and y-intercept with p-value from the linear regression analysis under isometric and dynamic fatigue progression on three participants is given in Table I. It is observed that only under the isometric scenario, the slope values are close to 1 and the $y-$intercept values are close to 0 across three participants, which indicates a consistent fatigue indicating performance among different individuals. Overall, the R^2 value is 0.870 ± 0.026 under the isometric case, while it is 0.803 ± 0.048 under the dynamic case. Therefore, the results in Fig. 3 and Table I imply that when using US ERC as the secondary fatigue indicator, the isometric scenario is likely to show significantly better indicating performance than the dynamic scenario ($p = 0.015$).

Table I: Results summary of linear regression models between the US ERC normalization and dorsiflexion force normalization, and between the US ERC normalization and dorsiflexion angle normalization on three participants.

	Isometric ankle dorsiflexion			Dynamic ankle dorsiflexion		
Ankle joint	R^2 value	Slope ($p-$value)	$y-$intercept ($p-$value)	R^2 value	Slope ($p-$value)	$y-$intercept ($p-$value)
A1 Left	0.873	1.059 (<0.001)	-0.064 (0.098)	0.741	1.256 (<0.001)	-0.192 (0.077)
A1 Right	0.844	1.063 (<0.001)	-0.046 (0.153)	0.789	0.611 (<0.001)	0.331 (<0.001)
A2 Left	0.899	1.130 (<0.001)	-0.055 (0.487)	0.857	0.521 (<0.001)	0.421 (<0.001)
A2 Right	0.836	1.043 (<0.001)	0.026 (0.761)	0.857	0.778 (<0.001)	0.284 (0.306)
A3 Left	0.897	1.082 (<0.001)	-0.040 (0.487)	0.813	0.856 (<0.001)	0.320 (0.688)
A3 Right	0.869	1.075 (<0.001)	-0.044 (0.317)	0.759	0.913 (<0.001)	0.071 (0.084)

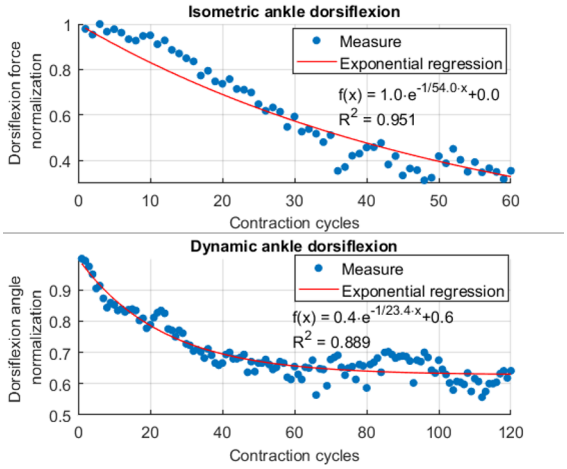

(a) Normalization of dorsiflexion force and angle decay relevant to TA muscle fatigue.

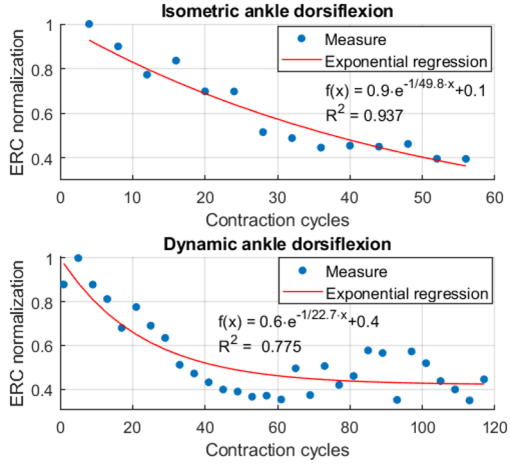

(b) Normalization of US ERC relevant to TA muscle fatigue.

Figure 2: The representative effects of FES-induced TA muscle fatigue on the dorsiflexion force normalization, dorsiflexion angle normalization, and US ERC normalization for both isometric and dynamic scenarios on Participant A1.

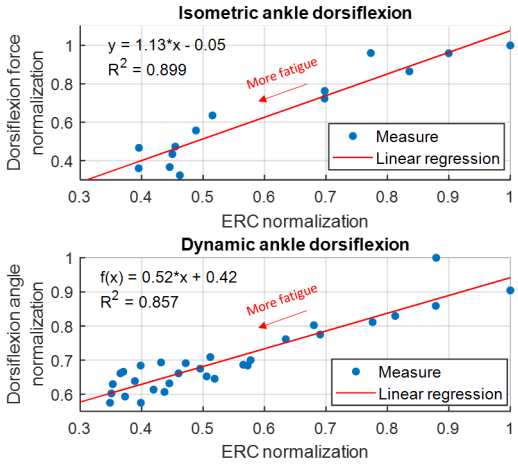

Figure 3: Relationships of the US ERC normalization vs. submaximal dorsiflexion force normalization and the US ERC vs. submaximal dorsiflexion angle normalization under isometric and dynamic FES-induced muscle fatigue progression periods. Reported data are from Participant A2.

The findings of the US imaging strain study in [28] showed that under the isometric case, the R^2 value of the linear regression model between submaximal mean (maximal) axial tissue strain and submaximal muscle force was 0.823±0.151 (0.850±0.165). The statistical analysis based on one-way repeated-measure ANOVA did not show any significant difference among three R^2 value groups ($p = 0.102$) for the isometric scenario, which indicates that US echogenicity is comparable to tissue strain as a muscle fatigue indicator. Furthermore, the computation times to get tissue strain and echogenicity in the same ROI were also calculated and compared based on a parallel computation framework, where the computation times per image frame were 0.795±0.261 ms and 368.714±7.168 ms for US echogenicity and tissue strain, respectively. Therefore, the advantages of using US echogenicity include: (1) the relatively robust selection of the ROI due to the static nature, (2) no requirement of US image with higher resolution and clearly visualized architectural features, (3) the significant reduction of calculation time (within 1 ms) for easier real-time implementation, and so on. The muscle force's or joint moment's decay during the FES-elicited muscle contraction has always been taken as a gold standard indicator for peripheral muscle fatigue, but measures of muscle force or joint moment usually require sophisticated hardware setup and are mainly constrained to isometric muscle contraction. Therefore, introducing an alternative non-invasive muscle fatigue indicator that can be easily implemented for both isometric and dynamic tasks, with a simpler setup and in a real-time manner, is necessary. Regarding features extraction from US imaging, the preliminary results showed that US echogenicity with easy access and simple calculation from US imaging is a prefer-

able real-time fatigue indicator during FES-induced muscle fatigue progression, which exhibits similar fatigue indication performance as previous methods such as strain imaging. Its main benefit in comparison to the strain imaging method is its quick computation time, which implies the potential implementations to assess muscle fatigue level during real-time FES rehabilitation training.

IV. Conclusion

The present study investigated the use of temporal US echogenicity from B-mode US images as the TA muscle fatigue candidate indicator during FES-induced isometric and dynamic ankle dorsiflexion motions. Synchronous measurements from isometric dorsiflexion force, dynamic dorsiflexion angle, and US images under the FES-induced muscle fatigue protocol were collected from both left and right ankle joints of three able-bodied participants. A computationally efficient gray-scaled analysis was used to determine if temporal ERC is correlated with the isometric dorsiflexion force ($R^2 = 0.870 \pm 0.026$) and dynamic dorsiflexion motion ($R^2 = 0.803 \pm 0.048$). The results of correlation analysis showed that the US echogenicity change was a comparable fatigue indicator to axial tissue strain during the isometric fatigue progression but with far-less computation time and high potentiality of real-time implementation. The findings in the current work indicate that, potentially, US echogenicity may be a promising non-invasive computationally efficient measure for assessing FES-induced muscle fatigue during neurorehabilitation implementations and can help with advanced FES controller design with the consideration of real-time muscle fatigue.

References

[1] M. E. Daubney and E. G. Culham, "Lower-Extremity Muscle Force and Balance Performance in Adults Aged 65 Years and Older," *Phys. Ther.*, vol. 79, no. 12, pp. 1177–1185, 1999.

[2] T. Killeen, C. S. Easthope, L. Demkó, L. Filli, L. Lőrincz, M. Linnebank, A. Curt, B. Zörner, and M. Bolliger, "Minimum toe clearance: probing the neural control of locomotion," *Sci. Rep.*, vol. 7, no. 1, pp. 1–10, 2017.

[3] M. H. Granat, D. J. Maxwell, A. C. Ferguson, K. R. Lees, and J. C. Barbenet, "Peroneal stimulator: Evaluation for the correction of spastic drop foot in hemiplegia," *Arch. Phys. Med. Rehabil.*, vol. 77, no. 1, pp. 19–24, 1996.

[4] G. Lyons, T. Sinkjaer, J. Burridge, and D. Wilcox, "A review of portable FES-based neural orthoses for the correction of drop foot," *IEEE Trans. Neur. Sys. and Rehab. Eng.,*, vol. 10, no. 4, pp. 260 –279, 2002.

[5] P. Melo, M. Silva, J. Martins, and D. Newman, "Technical developments of functional electrical stimulation to correct drop foot: sensing, actuation and control strategies," *Clin. Biomech.*, vol. 30, no. 2, pp. 101–113, 2015.

[6] N. Sharma, N. A. Kirsch, N. A. Alibeji, and W. E. Dixon, "A Non-Linear Control Method to Compensate for Muscle Fatigue during Neuromuscular Electrical Stimulation," *Front. Robot. AI*, vol. 4, p. 68, 2017.

[7] N. K. Vøllestad, "Measurement of human muscle fatigue," *J. Neurosci. Methods*, vol. 74, no. 2, pp. 219–227, 1997.

[8] T. Sadoyama and H. Miyano, "Frequency analysis of surface emg to evaluation of muscle fatigue," *Eur. J. Appl. Physiol. Occupational Physiol.*, vol. 47, no. 3, pp. 239–246, 1981.

[9] M. Cifrek, V. Medved, S. Tonković, and S. Ostojić, "Surface emg based muscle fatigue evaluation in biomechanics," *Clin. Biomech.*, vol. 24, no. 4, pp. 327–340, 2009.

[10] D. R. Rogers and D. T. MacIsaac, "Emg-based muscle fatigue assessment during dynamic contractions using principal component analysis," *J. Electromyogr. Kinesiol.*, vol. 21, no. 5, pp. 811–818, 2011.

[11] M. O. Ibitoye, N. A. Hamzaid, J. M. Zuniga, and A. K. A. Wahab, "Mechanomyography and muscle function assessment: A review of current state and prospects," *Clin. Biomech.*, vol. 29, no. 6, pp. 691–704, 2014.

[12] Y. Yoshitake, H. Ue, M. Miyazaki, and T. Moritani, "Assessment of lower-back muscle fatigue using electromyography, mechanomyography, and near-infrared spectroscopy," *Eur. J. Appl. Physiol.*, vol. 84, no. 3, pp. 174–179, 2001.

[13] M. Praagman, H. Veeger, E. Chadwick, W. Colier, and F. Van Der Helm, "Muscle oxygen consumption, determined by nirs, in relation to external force and emg," *J. Biomech.*, vol. 36, no. 7, pp. 905–912, 2003.

[14] M. J. Dawson, D. Gadian, and D. Wilkie, "Muscular fatigue investigated by phosphorus nuclear magnetic resonance," *Nature*, vol. 274, no. 5674, pp. 861–866, 1978.

[15] E. Ambrosini, S. Ferrante, T. Schauer, C. Klauer, M. Gaffuri, G. Ferrigno, and A. Pedrocchi, "A myocontrolled neuroprosthesis integrated with a passive exoskeleton to support upper limb activities," *J. Electromyogr. Kinesiol.*, vol. 24, no. 2, pp. 307–317, 2014.

[16] R. Pilkar, M. Yarossi, A. Ramanujam, V. Rajagopalan, M. B. Bayram, M. Mitchell, S. Canton, and G. Forrest, "Application of empirical mode decomposition combined with notch filtering for interpretation of surface electromyograms during functional electrical stimulation," *IEEE Trans. Neural Sys. Rehabil. Eng.*, vol. 25, no. 8, pp. 1268–1277, 2016.

[17] F. Mandrile, D. Farina, M. Pozzo, and R. Merletti, "Stimulation artifact in surface emg signal: effect of the stimulation waveform, detection system, and current amplitude using hybrid stimulation technique," *IEEE Trans. Neural Sys. Rehabil. Eng.*, vol. 11, no. 4, pp. 407–415, 2003.

[18] Z. Li, D. Guiraud, D. Andreu, M. Benoussaad, C. Fattal, and M. Hayashibe, "Real-time estimation of fes-induced joint torque with evoked emg," *J. Neuroeng. Rehabil.*, vol. 13, no. 1, p. 60, 2016.

[19] D. L. Crouch, L. Pan, W. Filer, J. W. Stallings, and H. Huang, "Comparing Surface and Intramuscular Electromyography for Simultaneous and Proportional Control Based on a Musculoskeletal Model: A Pilot Study," *IEEE Trans. Neural Syst. Rehabil. Eng.*, vol. 26, no. 9, pp. 1735–1744, 2018.

[20] J. Shi, Y.-P. Zheng, X. Chen, and Q.-H. Huang, "Assessment of muscle fatigue using sonomyography: muscle thickness change detected from ultrasound images," *Med. Eng. Phys.*, vol. 29, no. 4, pp. 472–479, 2007.

[21] R. S. Witte, K. Kim, B. J. Martin, and M. O'Donnell, "Effect of fatigue on muscle elasticity in the human forearm using ultrasound strain imaging," in *Proc. IEEE Int. Conf. Eng. Med. Biol. Soc.* IEEE, 2006, pp. 4490–4493.

[22] Z. Sheng, N. Sharma, and K. Kim, "Quantitative assessment of changes in muscle contractility due to fatigue during nmes: An ultrasound imaging approach," *IEEE Trans. Biomed. Eng.*, vol. 67, no. 3, pp. 832–841, 2019.

[23] S. Sikdar, H. Rangwala, E. B. Eastlake, I. A. Hunt, A. J. Nelson, J. Devanathan, A. Shin, and J. J. Pancrazio, "Novel method for predicting dexterous individual finger movements by imaging muscle activity using a wearable ultrasonic system," *IEEE Trans. Neural Syst. Rehabil. Eng.*, vol. 22, no. 1, pp. 69–76, 2013.

[24] Q. Zhang, A. Iyer, K. Kim, and N. Sharma, "Evaluation of non-invasive ankle joint effort prediction methods for use in neurorehabilitation using electromyography and ultrasound imaging," *IEEE Trans. Biomed. Eng.*, vol. 68, no. 3, pp. 1044–1055, 2021.

[25] Q. Zhang, K. Kim, and N. Sharma, "Prediction of Ankle Dorsiflexion Moment by Combined Ultrasound Sonography and Electromyography," *IEEE Trans. Neural Syst. Rehabil. Eng.*, vol. 28, no. 1, pp. 318–327, 2020.

[26] N. Kirsch, N. Alibeji, and N. Sharma, "Nonlinear model predictive control of functional electrical stimulation," *Control Eng. Practice*, vol. 58, pp. 319–331, 2017.

[27] O. R. Seynnes and N. J. Cronin, "Simple muscle architecture analysis (sma): An imagej macro tool to automate measurements in b-mode ultrasound scans," *Plos one*, vol. 15, no. 2, p. e0229034, 2020.

[28] Z. Sheng, N. Sharma, and K. Kim, "Ultra-high-frame-rate ultrasound monitoring of muscle contractility changes due to neuromuscular electrical stimulation," *Ann. Biomed. Eng.*, pp. 1–14, 2021.